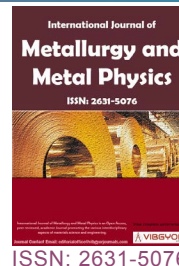


Modeling Digital Dual-Phase Structures



EA Bonifaz*

Department of Mechanical Engineering, Universidad San Francisco de Quito, Ecuador

Keywords

Heterogeneous materials, Digital structures, Constitutive behaviour, Cement paste, Aggregates, Inclusions, Nickel-base alloys

Introduction

A 3D finite element model was developed to simulate the influence of secondary phases (precipitates or aggregates) on the inelastic stress-strain distribution of nickel-based alloys and concrete structures. In both situations, the digital microstructure code DREAM.3D [1] was coupled to ABAQUS® finite element code through a MatLab® program. Representative Volume Elements (RVEs) of similar edge size but different inclusion (aggregate) size, morphology and distribution generated with DREAM.3D were tested with ABAQUS to investigate the relation between micro (and/or meso) and macro deformation and stress variables. The virtual specimens subjected to continuous monotonic strain loading conditions, were constrained with 3D boundary conditions (see Figure 1). *In the case of dual-phase polycrystalline nickel-based alloys*, the random polycrystalline aggregates generated with the software DREAM.3D have a constant volume fraction ratio [70% (matrix phase) - 30% (precipitate phase)]. The difference in crystallographic orientation, which evolves in the process of straining, and the incompatibility of deformation between

neighbouring grains were accounted for the evolution of geometrically necessary dislocation density, by the introduction of averaged Taylor factors, averaged young's modulus and single phase elastic limit through the strain hardening model documented in references [2,3]. *In the case of concrete structures* consisting of aggregates and hydrated cement paste, individual experimental curves in compression and tension documented in Bonifaz, et al. [4] were considered in the nonlinear analysis.

The effects of the phase type, inclusion size, morphology and distribution upon the composite (nickel alloy) local response are clearly observed in Figure 2 and Figure 3.

The elements considered in the analysis are also shown on the right. Stress units in $\frac{N}{\mu m^2}$. Element size = 1 μm . Element type C3D8.

Figure 3 shows the stress-strain curves for the documented element number in the four representative digital microstructures stated in Figure 2. Results reveal that the independent mechanical behavior of the analyzed element is affected by the phase type, inclusion size, distribution and mor-

*Corresponding author: EA Bonifaz, Department of Mechanical Engineering, Universidad San Francisco de Quito, Quito, Ecuador, Tel: 59322971700

Accepted: January 28, 2019; Published: January 30, 2019

Copyright: © 2019 Bonifaz EA. This is an open-access article distributed under the terms of the Creative Commons Attribution License, which permits unrestricted use, distribution, and reproduction in any medium, provided the original author and source are credited.

Bonifaz. Int J Metall Met Phys 2019, 4:028

ISSN 2631-5076



9 772631 507005

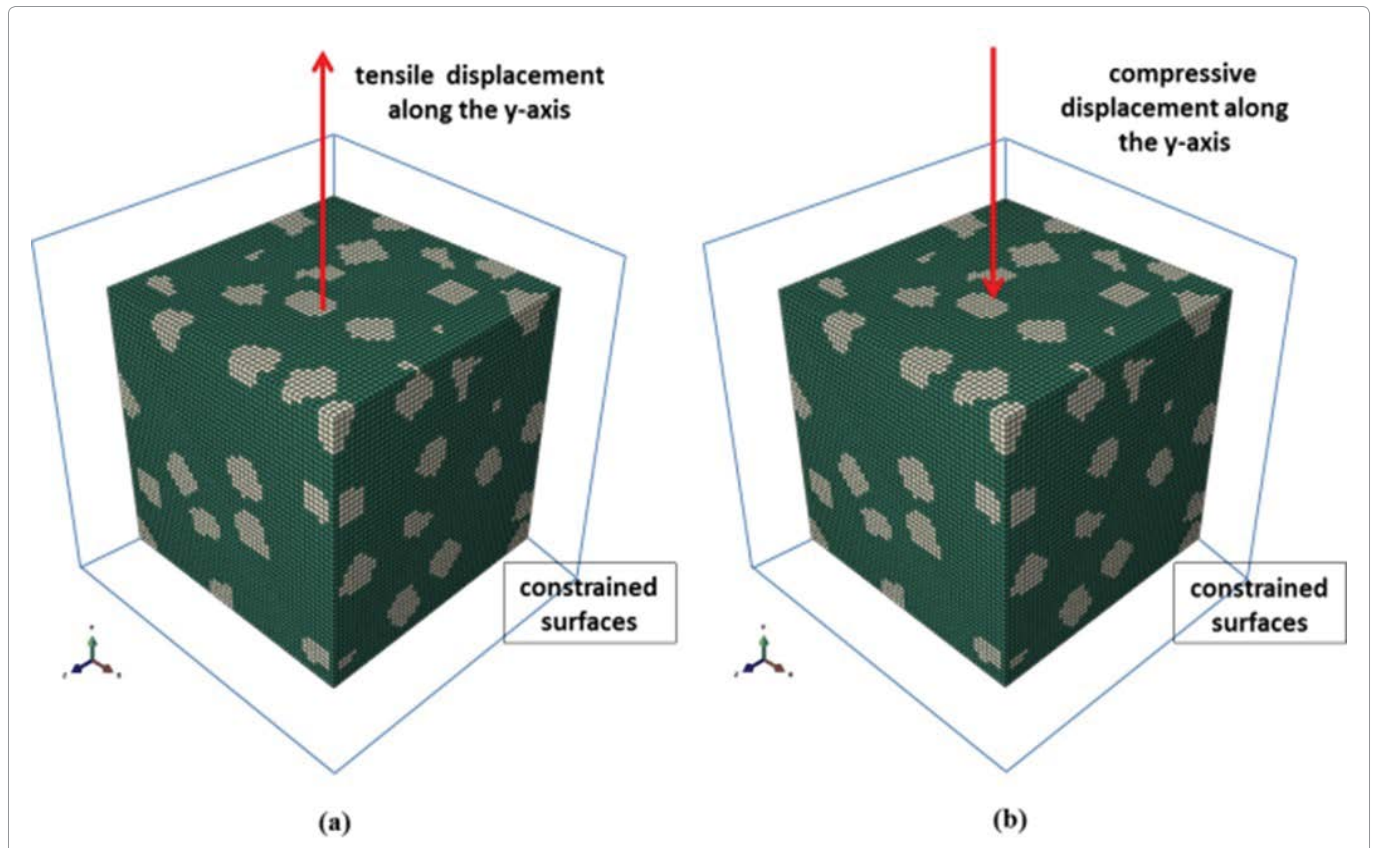


Figure 1: A dual-phase RVE constrained with 3D boundary conditions and subjected to continuous monotonic strain loading applied on the top face along the y-axis. a) Tension; b) Compression.

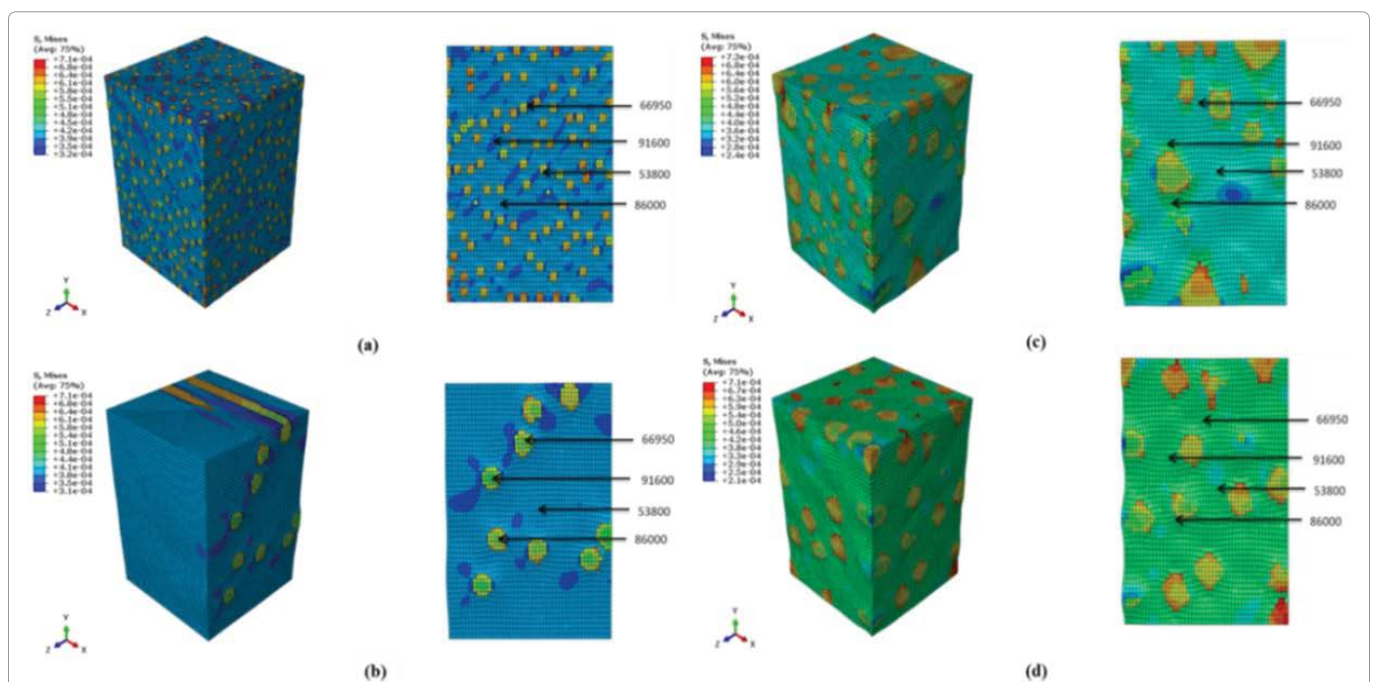


Figure 2: Von Mises stress contours for a 50 micron RVE dual-phase nickel-based alloy under displacement loading along the y-axis. a) RVE 1; b) RVE 2; c) RVE 3; d) RVE 4.

phology. The resistance to flow is higher in structures composed of finer and homogeneous spherical and/or cylindrical precipitates because the mis-

es stresses and effective plastic strains are better distributed. A strong dependence of flow stress and plastic strain on phase type, inclusion size, shape

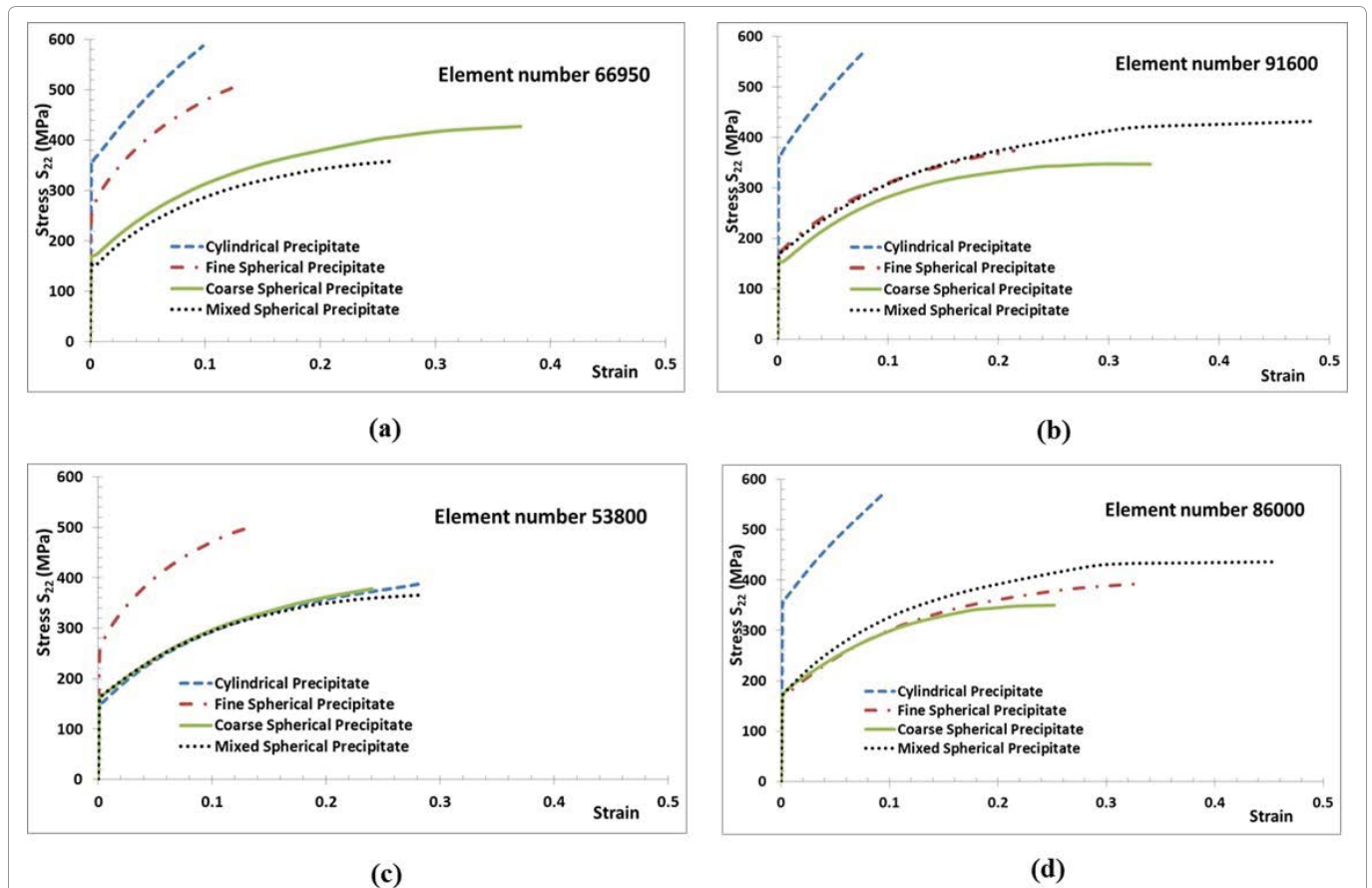


Figure 3: Element stress-strain curves obtained in the four RVEs subjected to displacement loading along the y-axis. a) For element number 66950; b) For element number 91600; c) For element number 53800; d) For element number 86000.

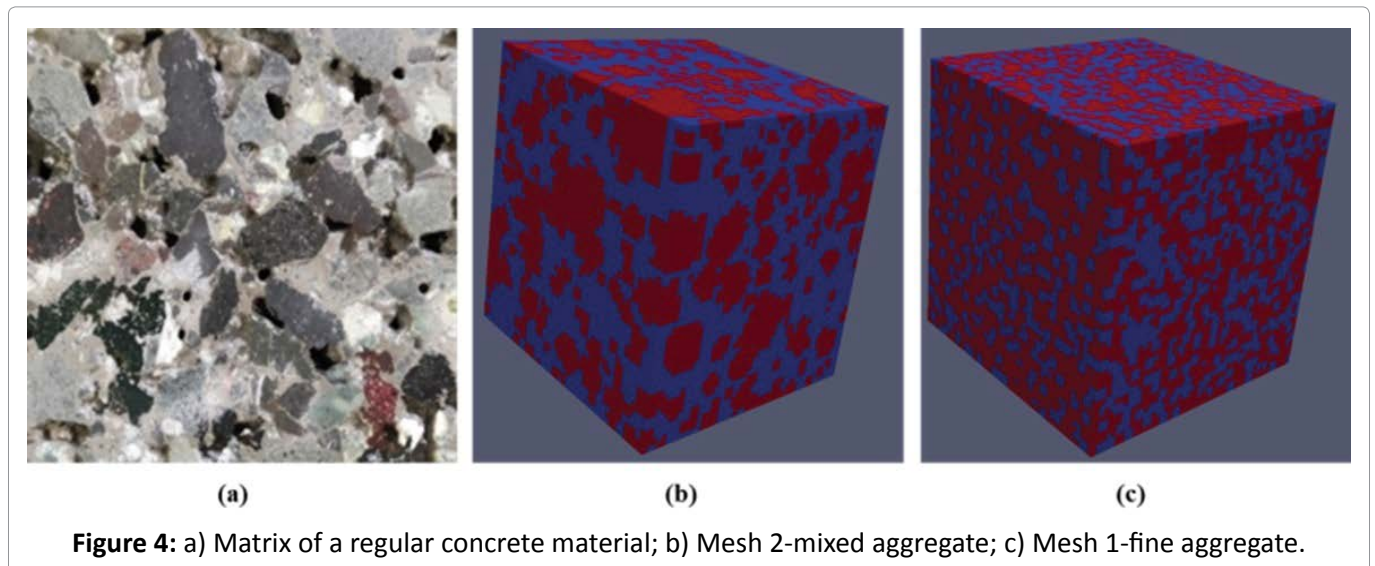


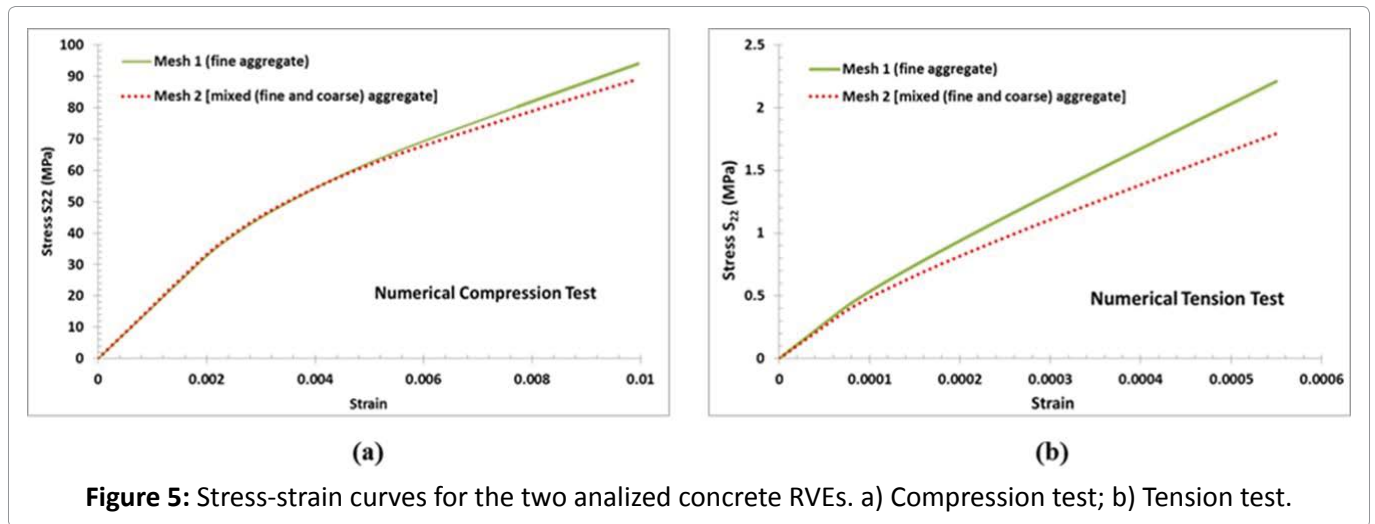
Figure 4: a) Matrix of a regular concrete material; b) Mesh 2-mixed aggregate; c) Mesh 1-fine aggregate.

and distribution are shown in Figure 2 and Figure 3. The effect of plastic deformation gradients imposed by the microstructure is clearly observed.

Element numbers documented in Figure 2 are located in the right surface of the cube.

Two affordable computational dual-phase (30%

matrix phase + 70% aggregates phase) representative volume elements used in the analysis of concrete meso-structures are shown on Figure 4. The structure in Figure 4b matches much better the matrix of concrete material presented in Figure 4a. Note that the fraction of air has been left out in the digital meso-structure.



Cubic box edge size $l_0 = 100$ mm, element size = 2 mm, element type C3D8.

The results of Figure 5 are in agreement with the expected output that the flow resistance is higher for structures composed of finer and homogeneously distributed inclusions (or aggregates).

References

1. M Groeber, M Jackson (2014) Integrating materials and manufacturing innovation. Springer Open Journal 3-5.
2. EA Bonifaz, NL Richards (2008) The plastic deformation of non-homogeneous polycrystals. Int J Plasticity 24: 289-301.
3. EA Bonifaz, J Baus, A Czekanski (2016) Finite element modelling of dual-phase polycrystalline nickel-base alloys. Mechanics of Materials 98: 134-141.
4. EA Bonifaz, J Baus, Eva OL Lantsoght (2017) Modeling concrete material structure: A two-phase meso finite element model. Journal of Multiscale Modelling 8: 1750004.